Measurement 223 (2023) 113780

Contents lists available at ScienceDirect

Measurement

journal homepage: www.elsevier.com/locate/measurement

Measurement and enhancing prediction of EPBM torque using actual Machine data

Ali Koohsari [a], Roohollah Kalatehjari [b,*], Sayfoddin Moosazadeh [c,**], Mohsen Hajihassani [c], Mostafa Tarafrava [d]

[a] Parhoon Tarh Co., 1531764511 Tehran, Iran
[b] Built Environment Engineering Department, School of Future Environments, Auckland University of Technology, Auckland 1010, New Zealand
[c] Department of Mining Engineering, Faculty of Engineering, Urmia University, 5756151818 Urmia, Iran
[d] Department of Mining Engineering, Amirkabir University of Technology, 15875-4413 Tehran, Iran

ARTICLE INFO

Keywords:
Mechanized tunneling
EPBM
Performance Prediction
Cutterhead Torque

ABSTRACT

The cutterhead torque of an Earth Pressure Balance Machine (EPBM) plays a critical role in determining the performance of mechanized tunneling in urban areas. However, as this parameter is not directly set by the operator but is a function of geological conditions, thrust force, screw conveyor revolution speed, and soil conditions, it is closely linked to geotechnical parameters and machine settings. Despite previous attempts to predict EPBM torque using Shi's physical model, accuracy has been lacking. This study aims to improve the accuracy of this prediction by utilizing actual data from an EPBM used in a metro line tunneling project to identify the primary factors influencing torque and to modify related equations accordingly. To evaluate the performance of existing models and the predictions made by the presented method, various metrics are utilized, including the correlation between all torque values, the relationship between torque and thrust values, and the connection between thrust pressure and penetration. The results indicate that in addition to geotechnical parameters, machine settings such as thrust force, cutterhead revolution speed, arching pressure, soil conditions, and chamber pressure significantly impact the torque value. The study found that the thrust force exerted by the EPBM is a key factor influencing torque.

1. Introduction

Mechanized tunneling has become a widely adopted approach for urban infrastructure development due to its ability to meet project timelines and costs while providing tunnel stability during excavation. The use of Earth Pressure Balance Machines (EPBM), in particular, allows for the real-time monitoring and balancing of earth pressure, thus minimizing the risk of surface settlement and subsurface deformations [8,17]; N. [29].

In context of EPBM operation, it is essential to differentiate between direct parameters (control parameters) and indirect parameters (response parameters) [19]. Direct parameters, which include thrust, cutterhead rotational speed, chamber pressure, and injection rates, are under the direct control of the TBM operator. On the other hand, response parameters, such as cutterhead torque, working pressure, face pressure, penetration, and advance speed, are influenced by ground conditions and the chosen control parameters [18,20].

Given the pivotal role of cutterhead torque as a crucial response parameter, as highlighted by Ates, Bilgin, and Copur [3], it becomes evident that operator cannot directly control this parameter. Therefore, the accurate prediction of cutterhead torque becomes essential in advancing the machine, which, in turn, critically impacting the device's design. Consequently, there is a clear and pressing need for the development of a reliable torque prediction method.

Several models, such as Bruland [7],Cigla and Ozdemir [9],Rostami and Ozdemir [23],Zare Naghadehi, Samaei, Ranjbarnia, and Nourani [28], and An et al. [1] have been established to predict parameters such as cutterhead torque under different rock mass conditions for hard rock TBM tunneling. They establish a correlation between machine performance parameters and geological rock mass traits. Additionally, several

* Corresponding authors.
** Corresponding authors.
E-mail addresses: ali.koohsari@gmail.com (A. Koohsari), r.kalatehjari@aut.ac.nz (R. Kalatehjari), s.moosazadeh@urmia.ac.ir (S. Moosazadeh), m.hajihassani@urmia.ac.ir (M. Hajihassani), mosy22@aut.ac.ir (M. Tarafrava).

https://doi.org/10.1016/j.measurement.2023.113780
Received 30 April 2023; Received in revised form 17 September 2023; Accepted 26 October 2023
Available online 2 November 2023

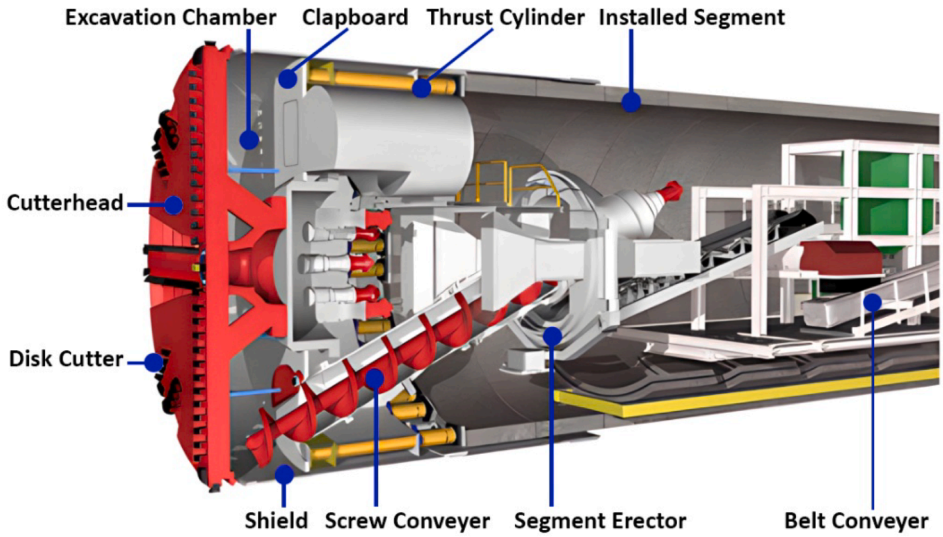

Fig. 1. Structure of the EPB shield machine [24].

researchers have forecasted cutterhead torque under mixed-face geological conditions based on varied rock properties [25,32,33]. However, EPBMs have undergone predictive studies to predict machine performance, with a particular focus on cutterhead torque in various soil conditions.

Krause [16] introduced an empirical formula shown in Equation (1) to calculate cutterhead torque based on numerous TBM projects. This formula correlates cutterhead torque with the cutterhead diameter, overlooking the geological conditions and other parameters. It is frequently used in cutterhead designs.

$$T_{(kN.m)} = \alpha D^3 \quad (1)$$

Where, D is cutterhead diameter (m), and α is an empirical coefficient between 9 and 25.

Subsequently, Korbin [15] suggested a theoretical model to predict cutterhead torque when the chamber is half full, factoring in geotechnical soil parameters and diameter as influences on the predicted torque [6]. Furthering this, Wittke, Erichsen, and Gattermann [27] introduced a formula shown in Equation (2) that decomposes the cutterhead torque into three components.

$$T_P = T_C + T_S + \Delta T \quad (2)$$

Where; T_P is the total torque, T_C is the torque of cutting tools, T_S is the torque of the friction against the cutterhead, and ΔT involves other components of torque.

Research by Melis Maynar [21] proposed that the cutterhead torque of cutting tools in the soil is less than 1 %. This value aligns with findings by González, Arroyo, and Gens [12], from data compiled from the Barcelona metro, which revealed that while cutting in rock, the torque of cutting tools reached up to 40 %, but in soil, it was less than 2 %.

The Japanese Society of Civil Engineering Standard Handbook[14] defines the various components that make up the cutterhead torque of an Earth Pressure Balance Machine (EPBM) comprising of the torque required to overcome the cutting resistance of the soil, the frictional resistance of the soil, the resistance of the soil mixing and stirring, the resistance of the main bearing, the frictional resistance of the cutter drive unit seal, and the mechanical losses in the reduction gears. The total of these components represents the cutterhead torque.

Shi, Yang, Gong, and Wang [24] introduced an analytical method based on a physical model as shown in Equation (3) to predict machine torque by dividing the cutterhead torque into eight components.

$$T = T_1 + T_2 + T_3 + T_4 + T_5 + T_6 + T_7 + T_8 \quad (3)$$

Where, T is the total torque of the cutterhead, T_1 is the frictional torque on the front surface of the cutterhead, T_2 is the frictional torque on the perimeter surface of the cutterhead, T_3 is the frictional torque on the back surface of the cutterhead, T_4 is the torque created by the cutting tools, T_5 is the shearing torque on the cutterhead openings, T_6 is the torque created by the mixing bars, T_7 is the torque to overcome the frictional resistance of the cutter drive unit seal, and T_8 is the main bearing torque.

Further investigations found T_1 to be the principal component, contributing to 40 % of the total torque, while T_3, T_7, and T_8 were deemed negligible with a combined contribution of less than 1 %. Zhou and Zhai [33] later identified two underlying assumptions of Shi's model, leading to its applicability only for EPBMs operating in soil, not mixed soils. Several modifications have been made to Shi's model, addressing its limitations, but no reference was made to soil cohesion, thrust force, or different soil conditions.

Wang, Gong, Shi, and Yang [26] tried to modify Shi's model regarding the start and end time of excavation (per ring) by considering the effect of penetration rate in T_1, and replacing overburden pressure with chamber pressure in some components. However, some limitations still exist in the modified model, with regards to constant diameter in the physical model and the absence of an arching effect. Godinez, Yu, Mooney, Gharahbagh, and Frank [11] made a further attempt to modify Shi's model by considering these limitations by replacing overburden pressure with chamber pressure and introducing a simple coefficient related to the soil disturbance and conditioning for all the main components of the original model. They concluded that the sum of T_1 and T_3 is over 60 %, and T_2 could not exceed 24 %.

Q. Zhang, Hou, Huang, Cai, and Kang [30] approached the cutterhead torque equation differently, considering nonlinear the pressure at the cutterhead front and the penetration rate's impact. Their model indicates a direct relationship between torque and penetration, but it only covers a few components Shi's model (i.e. T_1, T_4 and T_5) and misses out on necessary components, including the arching effect. Mooney et al. [22] also carried out an investigation and determined that in the low and mid-level range of the torque, there is a linear relationship between torque and penetration. Emre Avunduk and Copur [4] reviewed data from the Istanbul Ayvali Wastewater Tunnel and developed an empirical relationship between the geotechnical soil parameters and the cutterhead torque. The studied excavation was open, and the chamber was half full. The results showed that the torque in sandy soils is less than that of the high plasticity clayey soils. They also reported a decrease in the torque to the increase in moisture content of the soil. A similar result

Table 1
Specification of EPBM and the tunnel lining in the IML1.

Segment Parameters	Values
Internal diameter	6.0 *m*
Thickness	0.3 *m*
Ring Width	1.4 *m*
Cutterhead Parameters	**Values**
Diameter	6.9 *m*
Opening ratio	28 %
Thrust cylinders / Max force	19 pcs/32000 kN (315 bar)
Power/max torque	3 × 315 kW/4700 kN.m
Cutterhead rotational speed	0–4 rpm
Knives/Buckets	120/56 Pcs
Disc cutters	5 Pcs

was presented by Hu and Rostami [13]. In another study conducted on Mahmutbey Mecidiyekoy metro tunnels in Istanbul, E Avunduk et al. [5] reported that no relationship could be found between foam injection ratio (FIR), foam expansion ratio (FER), and torque.

While previous studies primarily focused on a limited number of factors influencing cutterhead torque in soil when using an EPBM, this study aims to develop a simplified equation for estimating cutterhead torque that considers thrust force, chamber pressure, arching pressure, cutterhead revolution speed, penetration rate, soil conditioning, and soil type. The main objective of this research is to establish a relationship between the response parameter, torque, and various direct parameters as introduced above. This relationship will assist designers, tunnel engineers, and coordinators of EPBM in determining torque by controlling direct parameters. Although this approach may lead to a more complex equation, it offers a more comprehensive understanding of the factors influencing cutterhead torque. This study is based on geological and machine data from Isfahan Metro Line 1 (IML1) and intends to present a modified cutterhead torque equation, highlighting thrust force, soil conditioning, chamber pressure, and arching effects as its principal parameters.

2. The Isfahan metro line 1 (IML1)

Isfahan Metro tunnels are excavated by Earth Pressure Balance Machine (EPBM). Fig. 1 shows the structure of the EPB shield machine. The IML1 connects the northwest of the city to the south. As shown in Fig. 1, about 5 km of this line has been excavated by two EPBMs as a twin tunnel (western and eastern). Details of the tunnel lining and the machines' specifications are listed in Table 1. This study utilizes the data collected from a 2 km length of this line, as highlighted in Fig. 1. Most of the tunnel is situated in sedimentary river deposits, which consist primarily of sand and gravel with some clay, as shown in the geological profile of the IMIL1 in Fig. 2. The geotechnical parameters for the soil along the tunnel route are listed in Table 2.

Table 2
Geotechnical parameters of soil in IML1.

Soil Type	Ring		ϕ	c
CI-CL	1402	1617	24	30
GM-GP	1617	1724	33	5
SP-SW	1724	1888	32	0
GP	1888	2074	29	5
GW	2074	2227	34	0
SP-SW	2227	2260	30	0
GP-GW	2260	2460	31	0
GM-GC	2460	2531	31	5
SP-SW	2531	2595	32	0
GM-GP	2595	2688	33	5
SP-SW	2688	2724	30	0
GM-GC	2724	2795	33	5

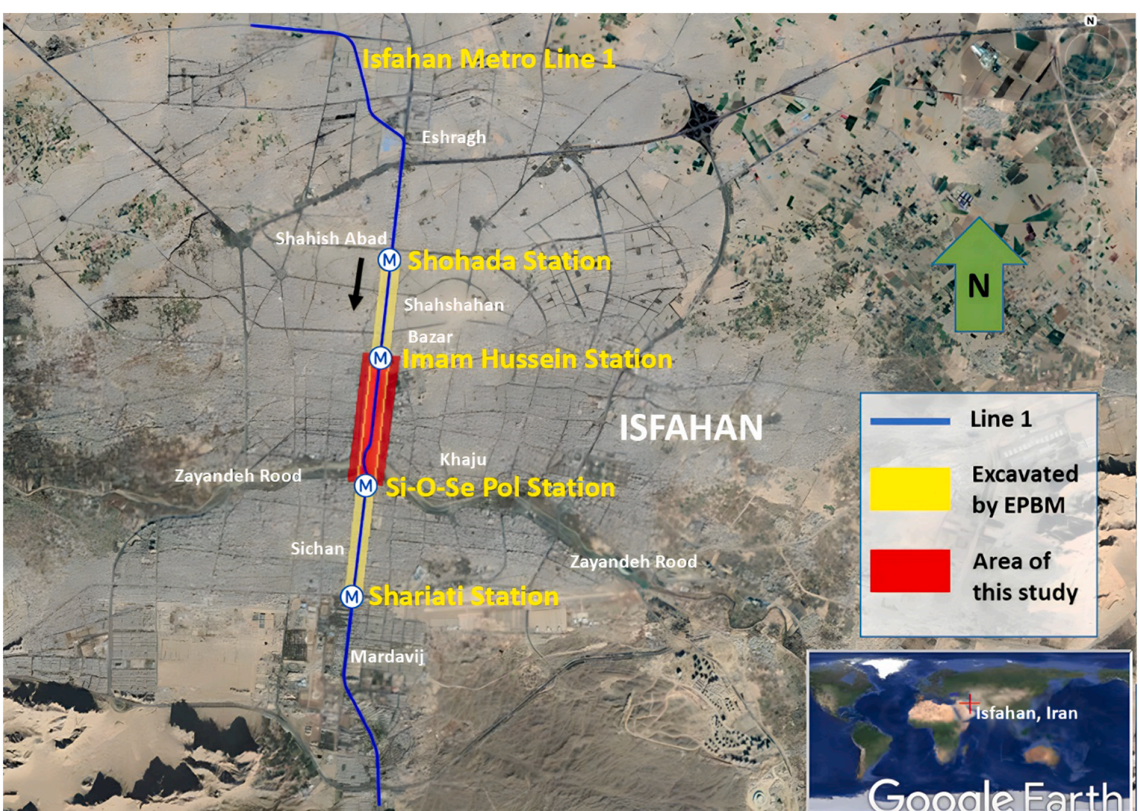

Fig. 2. The route of the IML1 (after Google Imagery @2022 CNES/Airbus, Maxar Technologies, Map Data @2022).

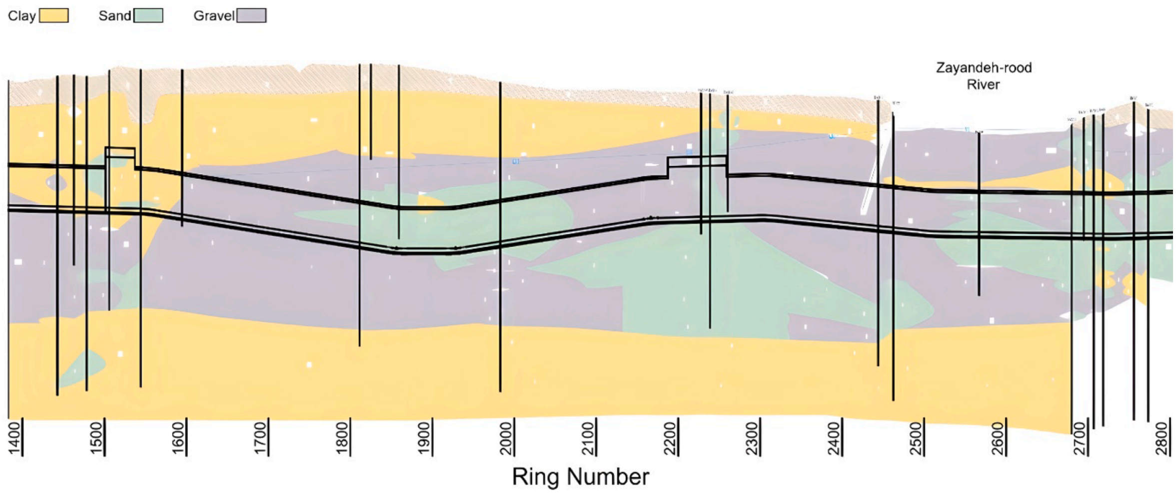

Fig. 3. Geological profile of the IML1 from ring 1400 to 2800 [10].

2.1. Excavation data of IML1

The excavation data from ring 1400 to ring 2800 of the IML1 was obtained from the data acquisition systems in both the western and eastern tunnels, as presented in Fig. 3. The data includes penetration rate, thrust force, cutterhead revolution speed, chamber pressure, screw rotational speed, arching pressure, and cutterhead torque. A review of the values from both tunnels shows that they are generally very similar, with marked differences between rings 1800 to 2100, where thrust force, cutterhead revolution speed, and chamber pressure in the eastern tunnel differ from the values in the western tunnel. However, the torque range is similar along both tunnels, which is believed to be caused by the EPBMs encountering the same soil layers with similar geotechnical parameters.

The operator's reaction to soil layer changes can be observed from the variation of penetration values. Typically, the operator has forced the machine to reach its maximum allowable torque in each soil type to have the maximum penetration rate. Consequently, the range of torque values in all soil types is almost the same. Hence, it is difficult to predict the penetration rate for the same torque for each soil type. As can be seen, different torque and penetration rates are recorded for the same soil types.

2.2. The modified model

Equation (4), containing five main components, was initially presented by Shi et al. [24] to predict the torque value and later modified by Godinez et al. [11].

$$T_{EPB} = T_1 + T_2 + T_3 + T_5 + T_6 \tag{4}$$

Where, T_{EPB} is the total cutterhead torque, and its components are derived from equations (5) to (9). The functional mechanism of torque components is presented in Fig. 4.

$$T_1 = \frac{\pi D^3}{12} P_1 \mu_1 (1 - \eta) \tag{5}$$

$$T_2 = \frac{\pi D^2}{2} P_2 \mu_2 t \tag{6}$$

$$T_3 = \frac{\pi D^3}{12} P_3 \mu_3 (1 - \eta) \tag{7}$$

$$T_5 = \frac{\pi D^3}{12} P_3 \mu_3 \eta k_q \tag{8}$$

$$T_6 = D_b L_b n_b R_b P_3 \mu_3 \tag{9}$$

In the components equations T_i s are torque components that were introduced in previous sections, D is the cutterhead diameter, P_i s are effective pressures for every component, μ_i s are the friction coefficient between the soil and every part of the cutterhead, η is the opening ratio of the cutterhead, t is the width of the cutterhead, k_q is a coefficient related to the shape of the openings, D_b is the diameter of the mixing bars, L_b is the length of the mixing bars, n_b is the number of mixing bars, and R_b is the distance between the bars and the centerline of the shield.

In Shi's[24] model, P_i values in all components are considered as the overburden pressure, but this is not a true assumption due to physical modeling limitations in real projects. Wang et al. [26] replaced P_i with the chamber pressure in some components to improve Shi's [24] model. Godinez et al. [11] replaced all P_i s with the chamber pressure and applied coefficients to intact soil parameters to better represent the disturbed and conditioned soil behavior. Even though each researcher improved Shi's model, they could not achieve comparative results to actual values due to the complexity of torque.

Fig. 5 compares predicted values from Godinez et al. [11] modified model and the actual torque values from the IML1, which offers a good prediction over specific tunnel sections. However, in the same ring, the torque value fluctuates over a wide range, and in clay soil, the predicted values are far from the actual values. Fig. 6 shows the correlation between all torque values and the R^2 is typically 0.03. These results suggest that Godinez et al. [11] model may miss some critical parameters. Therefore, further study of each component should be carried out to modify and improve the available models.

2.3. T_1 Component

This component represents friction torque on the front face of the cutterhead, which is the friction generated where the cutterhead openings do not exist. The main parameter to produce this torque component is the contact pressure between the front face of the cutterhead and the excavated soil. The cutterhead is forced to move forward by applying a thrust force, creating contact between the cutting tools and the intact soil. In such a situation, the chamber pressure is transferred to the face only through the openings. In other areas, the pressure on the face is related to the applied thrust force.

Considering a particular situation where the advance of the EPBM stops but the cutterhead continues to rotate, and a constant chamber pressure is applied, the torque value of Shi et al. [24] and Godinez et al. [11] equations will be stable because of the consistency formed in the chamber and the arching pressures. However, as seen in Fig. 7, the

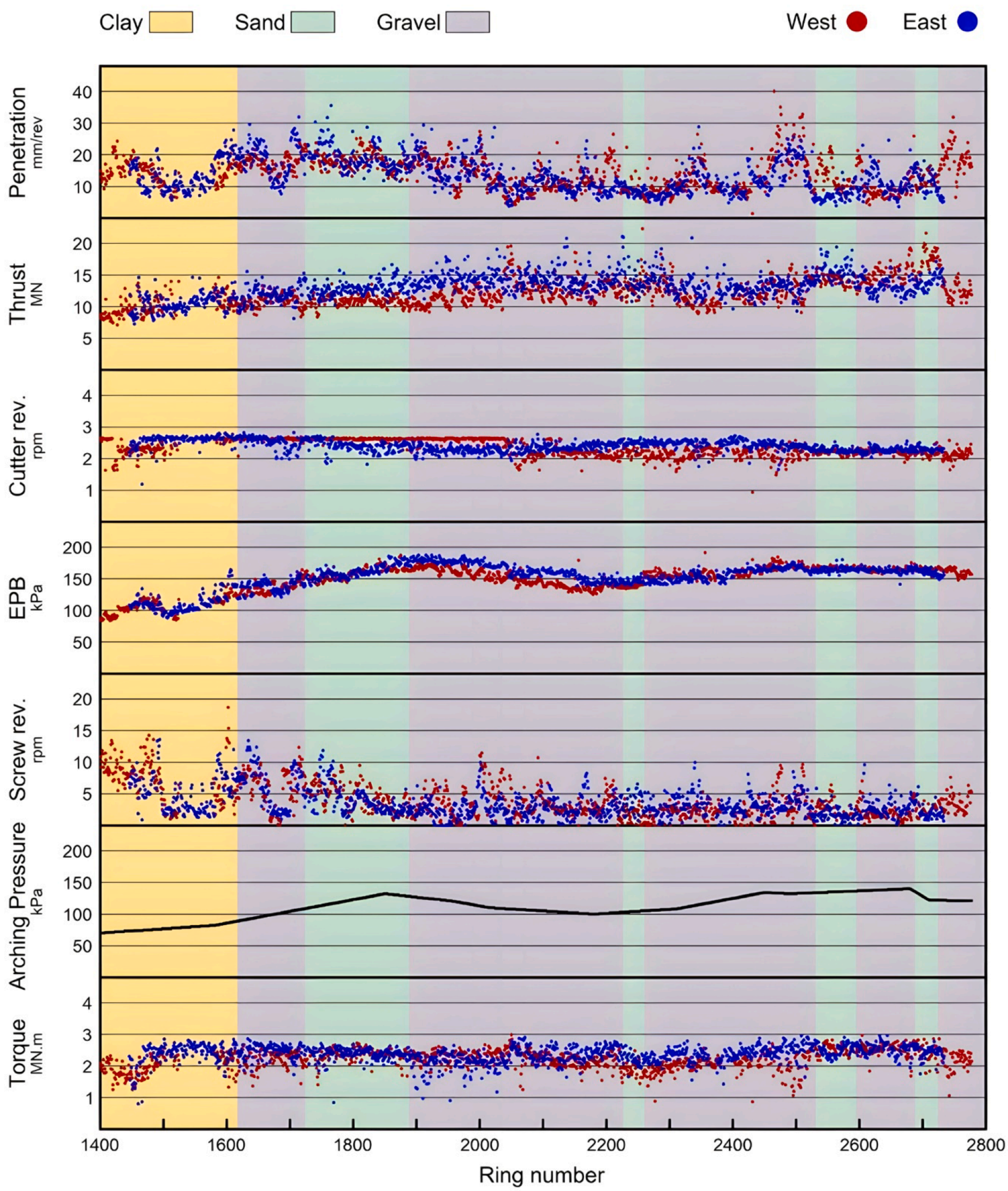

Fig. 4. EPBM Data of IML1.

actual torque value of the machine reduces significantly. The reduction in torque is due to a decrease in thrust force. Therefore, neither the pressure inside the chamber nor the arching pressure causes low or high pressure on the front face of the cutterhead, but the thrust force causes the torque.

Q. Zhang et al. [31] considered the components of the thrust force. With the deduction of friction forces generated by the shield, articulation, backup, and chamber reaction force, the net applied thrust force to the face can be calculated based on equation (10).

$$F_{face} = F_{total} - (F_{artiqulation} + F_{backup} + F_{friction} + F_{Chamber}) \quad (10)$$

Where, F_{total}, $F_{artiqulation}$ and F_{backup} can be directly derived from machine data. The rest of parameters should be calculated using equations (11) and (12).

$$F_{friction} = f(\pi D L P_2 + W) \quad (11)$$

$$F_{Chamber} = \frac{\pi D^2}{4} \eta P_3 \quad (12)$$

Where, f is the friction coefficient between the shield and the earth, L is the shield length, P_2 is the earth pressure ($P_{Arching}$), W is shield weight, and P_3 is the pressure inside the chamber ($P_{Chamber}$).

The mean pressure generated by F_{face} can be calculated by equation (13).

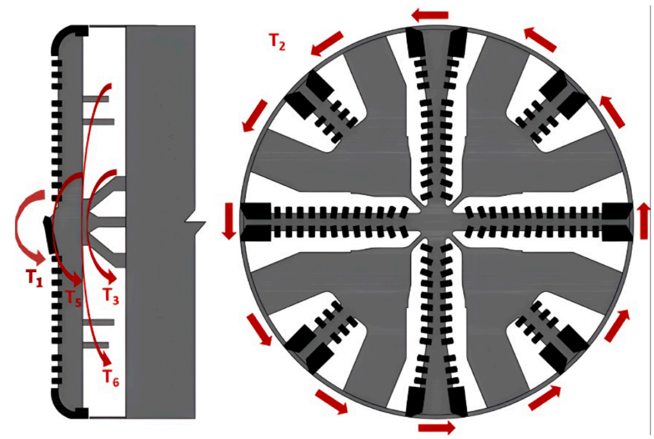

Fig. 5. Functional mechanism of torque components.

$$P_1 = \frac{F_{face}}{A} \tag{13}$$

Where, P_1 is the pressure generated by the thrust force to the front face of the cutterhead (P_{Thrust}), and A is the area of the cutterhead. Therefore, T_1 can be calculated by replacing P_1 in the equation (14).

$$T_1 = \frac{\pi D^3}{12} P_{Thrust} \mu_1 (1 - \eta) \tag{14}$$

Note that μ_1 coefficient, which is related to the geotechnical properties of soil, can be calculated as equation (15).

$$\mu_1 = f_1(\tan(\varphi) + c/P_{Chamber}) \tag{15}$$

Where, f_1 represents the situation of disturbance and condition of the soil in the tunnel face.

2.4. T_2 Component

This component represents the frictional torque on the perimeter surface of the cutterhead. Due to the small distance between the cutterhead perimeter and the earth, the pressure inside the chamber cannot be considered as the effective pressure on this zone; instead, the arching pressure is the effective force on the cutterhead perimeter, which can be calculated by the existing relations developed by Arthur et al. [2] amongst others. This component can be calculated as equation (16).

$$T_2 = \frac{\pi D^2}{2} P_2 \mu_2 t \tag{16}$$

Where, P_2 in the arching pressure ($P_{Arching}$), and μ_2 shows the friction value between the cutterhead perimeter and the earth, and μ_2 is obtained from equation (17).

$$\mu_2 = f_2(tan(\varphi) + c/P_{Arching}) \tag{17}$$

Where, f_2 represents the situation of disturbance and conditioned soil around the perimeter of the cutterhead.

2.5. T_3 And T_5 components

These two components have almost the exact functional mechanism. The effective pressure acting on them is the pressure inside the chamber. They also have a direct relationship with the diameter of the cutterhead, as shown by equations (18) and (19).

$$T_{3,5} = T_3 + T_5 = \frac{\pi D^3}{12} P_3 \mu_3 (1 - \eta) + \frac{\pi D^3}{12} P_3 \mu_3 \eta \, k_q \tag{18}$$

$$T_{3,5} = \frac{\pi D^3}{12} P_3 \mu_3 (1 - \eta + \eta \, k_q) \tag{19}$$

Where, D is the diameter of the cutterhead, P_3 is the pressure inside the chamber ($P_{Chamber}$), k_q is a coefficient related to the shape of the opening, and μ_3 is a coefficient related to the properties of conditioned soil, and μ_3 is obtained from equation (20).

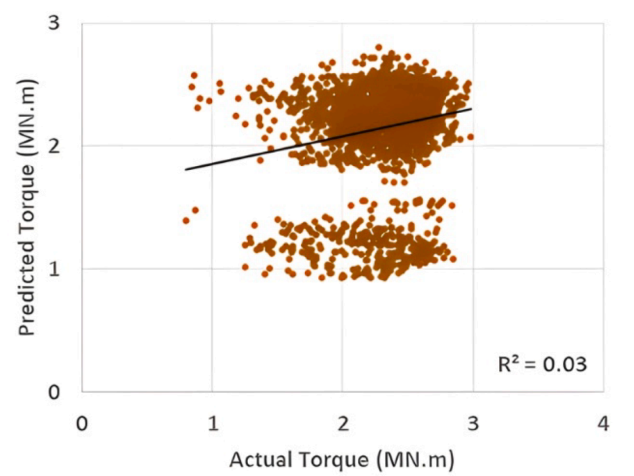

Fig. 7. Correlation between all torque values from IML1 and Godinez et al. [11] model.

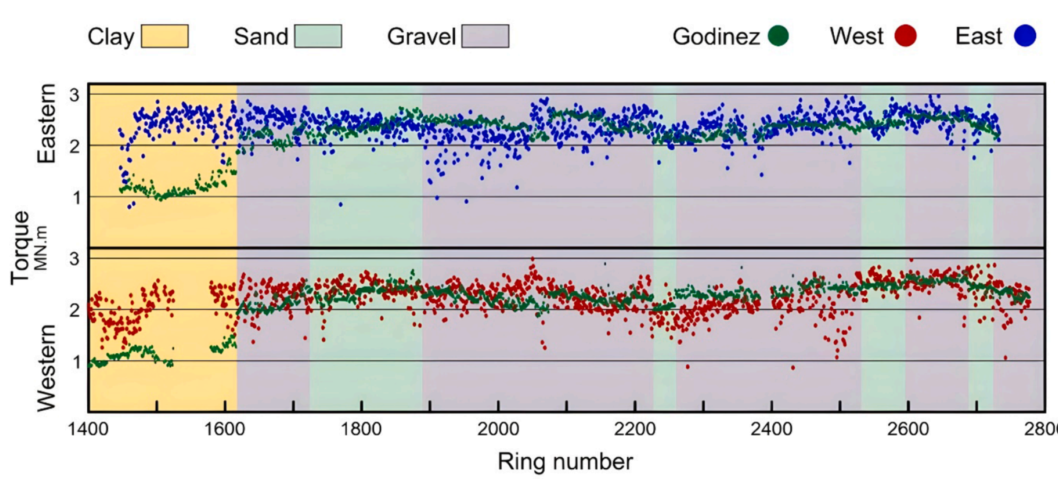

Fig. 6. Comparison of actual torque in IML1 and Godinez et al. [11] model.

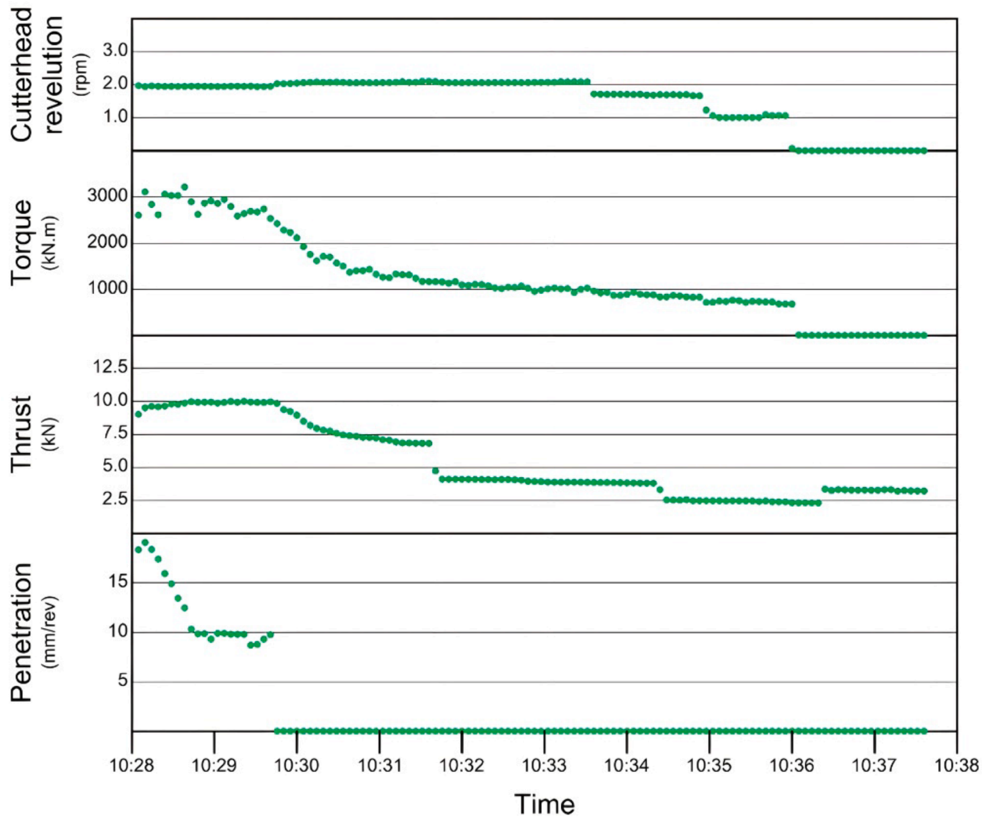

Fig. 8. Relation between the torque and thrust values.

$$\mu_3 = f_3(\tan(\varphi) + c/P_{Chamber}) \tag{20}$$

Where, f_3 represents the disturbed and conditioned soil inside the chamber.

It is evident that due to the different conditions of the soil in front of the cutterhead, around the cutterhead perimeter, and inside of the chamber, f_i values (Equations (15), 17, and 20) are not equal and always $f_3 < f_1 < f_2$.

2.6. Other components

Shi's model suggests that the sealing and bearing torque values are negligible, but this is not true. They are related to the state of the machine. As seen in Fig. 8, the torque value of the cutterhead when it was outside the tunnel before it was launched, and the chamber was empty was far from zero. As shown, the torque has a direct relationship with the revolution speed. With the cutterhead revolution speed at 2.0 rpm, the torque is 60 kN.m. The torque is reduced by reducing the rotational speed of the cutterhead. The rotational speed of the cutterhead is the summation of T_7 and T_8. The value of T_6 is only dependent on the pressure inside the chamber due to the constancy of the other parameters. The summation of these components based on Shi's and [21]'s calculations is less than 5 %. In this study, they are presented as T_{Other}. In conclusion, the total torque of the EPBM is equal to the sum of the previously mentioned components. In contracts with the findings of previous studies, torque, and rotational speed of the cutterhead have a direct relationship, as shown in Figs. 7 and 8. The values of f_1, f_2 and f_3 can be determined by performing linear regression analysis on EPBM

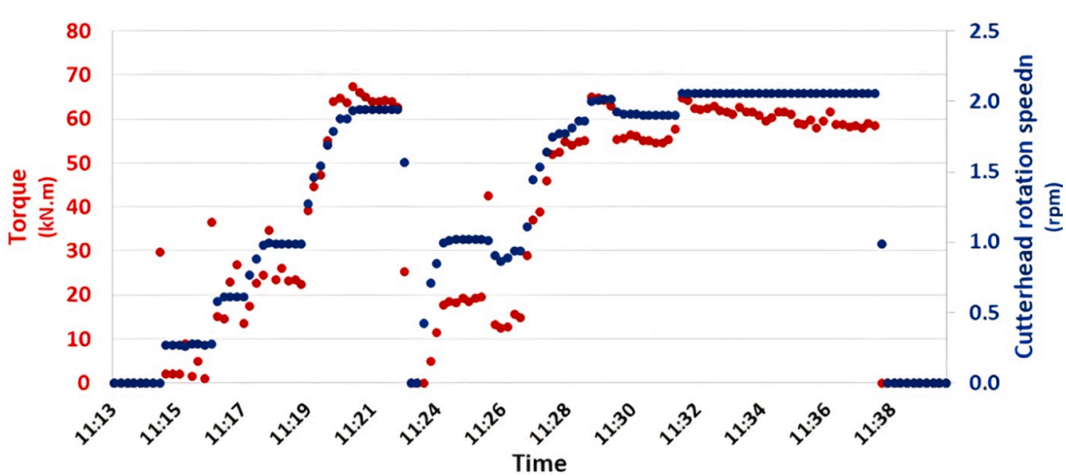

Fig. 9. Effect of RPM on torque value when EPBM is outside of the tunnel.

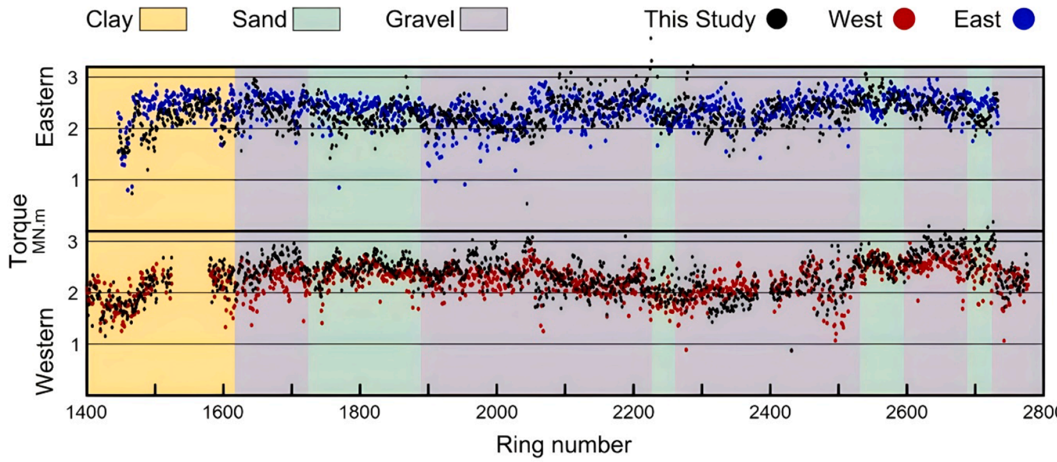

Fig. 10. Comparison of actual torque and this study modified model.

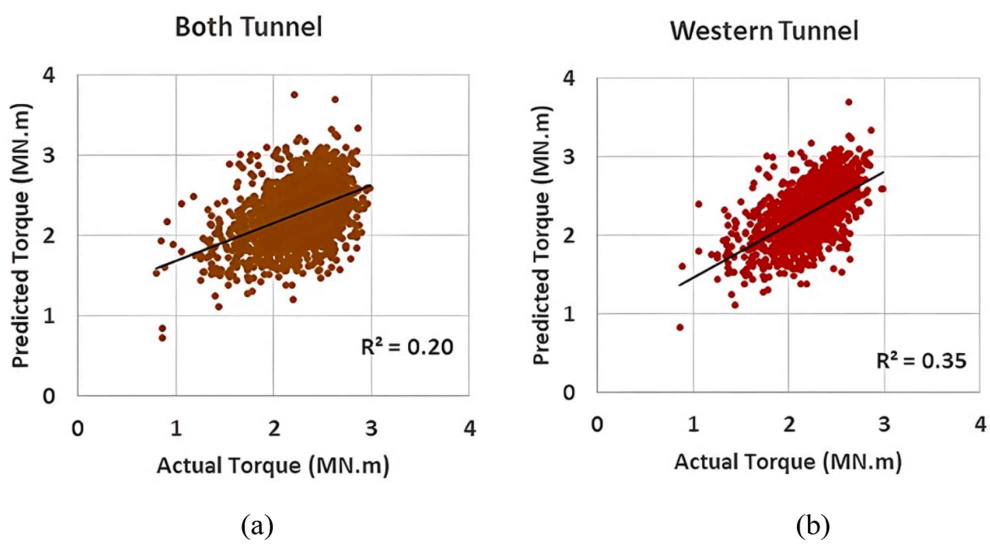

Fig. 11. Prediction by the presented method vs. actual torque values for (a) both tunnels and (b) western tunnels.

data based on the torque components equation. By summation of all T_i s, the torque is presented as equation (21).

$$T_{EPBM} = \omega(T_1 + T_2 + T_{3,5} + T_{Other}) \tag{21}$$

Where, T_{EPBM} is the total torque of the machine, ω is the rotational speed, and T_1, T_2, $T_{3,5}$ can be derived from Equations (14), 16, and 19, respectively.

3. Results

Based on the analysis of the IML1 machine and soil data, the f_i values are the only parameters calculated by linear regression on the torque equation. The calculated values are $f_1 = 0.17, f_2 = 0.22$, and $f_3 = 0.05$. Fig. 9 shows the results of the modified model value compared to the actual values for both the western and eastern tunnels. Soil parameters for the western tunnel are expected to be more accurate as most boreholes were drilled closer to that tunnel alignment. Therefore, the results of the western tunnel give more accurate torque values with R^2 value equal to 0.35 compared to an overall R^2 value for both tunnels equivalent to 0.20, as seen in Fig. 10. The components values based on the new modified model are $T_1 = 54\%$, $T_2 = 26\%$, $T_{3,5} = 15\%$, and $T_{Other} = 5\%$.

It is evident that T_1 accounts for about 54 % of total torque, and the value closely compares to the actual observed values. As shown in Fig. 7, the torque value decreases from 2.7 to 1.0 MN.m (about 63 %) after stopping the machine advancement, which is believed to be due to the reduction in the thrust force. The effect of penetration on torque, as presented by [20] and others, has not been discussed. There is a relationship between thrust force and penetration in the EPBM, as illustrated in Fig. 11. The average FPI (FPIA) shown in the figure is the thrust pressure (P_{Thrust}) divided by penetration. A strong relationship between FPIA and penetration is evident with $R^2 = 0.8$. Fig. 12.

The boreholes in IML1 are mainly focused near the stations, so the distance between the boreholes in some areas is about 200 rings (280 m). It is believed that if the borehole data were more closely aligned with the tunnels providing more accurate soil parameters, the correlations would be better, and the value of R^2 would be closer to 1.0. This theory is proven to be true as presented in Figs. 13 and 14 showing the results of ring 2447 where the borehole BH-60115 is close to the western tunnel, correlating with $R^2 = 0.84$.

The results of the proposed model demonstrate a significant degree of unity with the actual torque values, as evidenced by the substantial overlap in the range of predicted values for a specific tunnel length. This represents a marked improvement in the performance of previous methods.

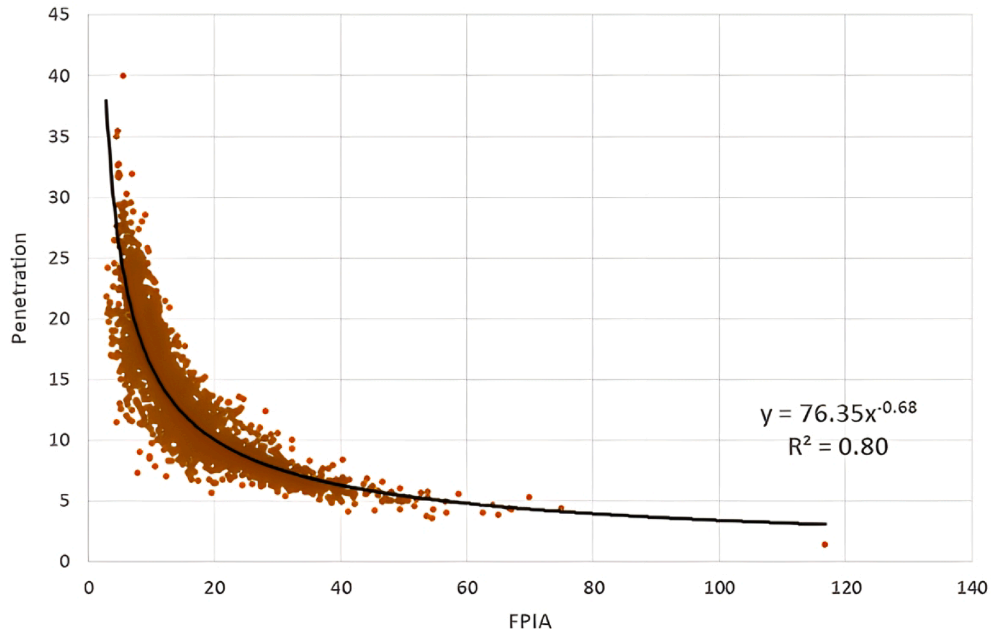

Fig. 12. The relationship between thrust pressure and penetration.

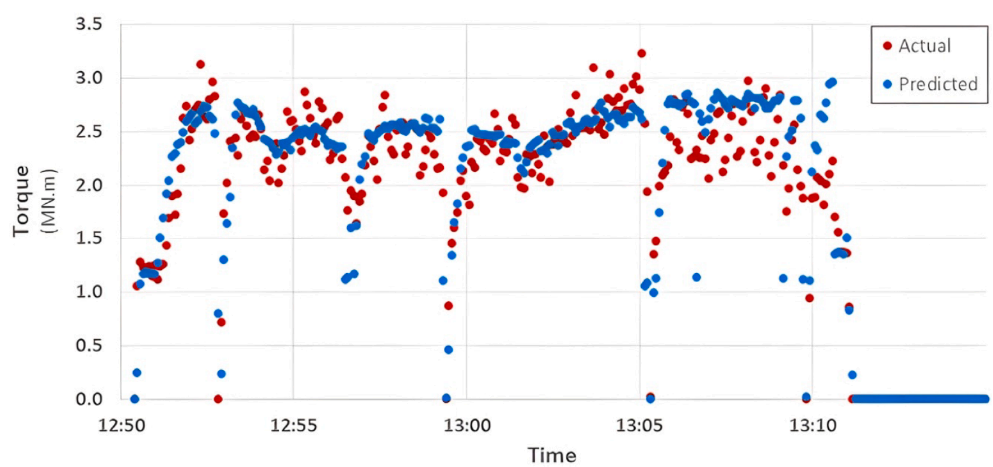

Fig. 13. Predicted and actual torque values at ring 2447 in the western tunnel.

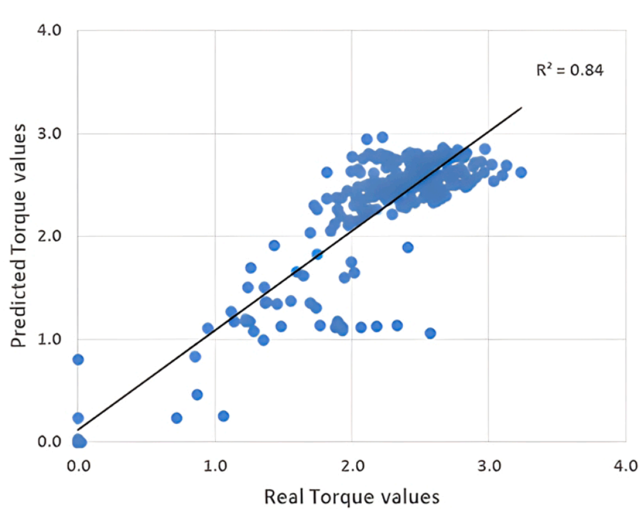

Fig. 14. Correlation of Predicted and actual torque values at ring 2447.

4. Results

This study detailed a comprehensive examination and modification of the torque generated by an Earth Pressure Balance Machine (EPBM) during tunneling operations. The findings underscored significant aspects in understanding the complex mechanisms behind torque generation and established a valuable contribution to this field. The key conclusions of our research can be summarized as follows:

- The study introduced a refined and modified equation for torque calculation. This new model enhanced our understanding of the torque generation process and gave a fresh perspective on its components.
- A direct relationship between torque and the cutterhead's rotational speed was discovered, demonstrating a key operational link within the EPBM's operation.
- The modified model's predictions were compared with the actual results, revealing varying degrees of correlation. An R^2 value of 0.20 was obtained for combined data from both tunnels, while data from the western tunnel alone resulted in an R^2 value of 0.35. This

difference can be tracked back to the enhanced precision of soil parameters for the western tunnel.

- The results for ring 2447, located close to the borehole BH-60115 is in the western tunnel, displayed a higher correlating with an R^2 value of 0.84, showing a strong link between the theoretical model and practical data.
- The thrust force exerted by the EPBM was identified as a significant factor influencing the generated torque, demonstrating the intricate interplay of forces at work during tunneling operations.
- A further breakdown of torque components showed that T_1, T_2, and $T_{3,5}$ contributed to 54 %, 26 %, and 15 % of the total torque value, respectively. Meanwhile, the remaining components collectively contributed a mere 5 % of the total torque value.

These findings conclude our comprehensive analysis of torque generation in EPBMs, offering both significant insights and practical value for further investigations in this domain.

CRediT authorship contribution statement

Ali Koohsari: Conceptualization, Methodology, Software, Formal analysis, Investigation, Resources, Writing – original draft, Visualization. **Roohollah Kalatehjari:** Methodology, Validation, Formal analysis, Writing – original draft, Writing – review & editing, Visualization, Supervision. **Sayfoddin Moosazadeh:** Conceptualization, Methodology, Software, Investigation, Writing – original draft, Supervision. **Mohsen Hajihassani:** Software, Validation, Formal analysis, Investigation, Resources, Writing – review & editing, Supervision. **Mostafa Tarafrava:** Software, Validation, Resources, Writing – review & editing.

Declaration of Competing Interest

The authors declare that they have no known competing financial interests or personal relationships that could have appeared to influence the work reported in this paper.

Data availability

The authors do not have permission to share data.

Acknowledgements

The authors extend their gratitude to the Isfahan Urban Railway Organization for providing the data used in this study.

References

[1] Y. An, Z. Li, C. Wu, H. Hu, C. Shao, B. Li, Earth pressure field modeling for tunnel face stability evaluation of EPB shield machines based on optimization solution, Discrete and Continuous Dynamical Systems: Series S 13 (6) (2020) 1721–1741.
[2] Arthur, L., Darby, A., Rafoneke, B., Daws, G., MacDonald, D., Innaurato, N., . . . Coutts, A. (1994). *Face support for a large mix-shield in heterogeneous ground conditions.* Paper presented at the Tunnelling'94: Papers presented at the seventh international symposium,'Tunnelling'94'.
[3] U. Ates, N. Bilgin, H. Copur, Estimating torque, thrust and other design parameters of different type TBMs with some criticism to TBMs used in Turkish tunneling projects, Tunn. Undergr. Space Technol. 40 (2014) 46–63.
[4] E. Avunduk, H. Copur, Empirical modeling for predicting excavation performance of EPB TBM based on soil properties, Tunn. Undergr. Space Technol. 71 (2018) 340–353.
[5] E. Avunduk, H. Copur, S. Tolouei, D. Tumac, C. Balci, N. Bilgin, A. Shaterpour –Mamaghani, Possibility of using torvane shear testing device for soil conditioning optimization, Tunn. Undergr. Space Technol. 107 (2021) 103665.
[6] N. Bilgin, H. Copur, C. Balci, Mechanical excavation in mining and civil industries CRC Press, Boca Raton (2014), p366.
[7] A. Bruland, Hard rock tunnel boring, Norwegian University of Science and Technology, Trondheim, Norway, 1998 [Ph. D. Thesis].
[8] R.-P. Chen, X.u. Song, F.-Y. Meng, H.-N. Wu, X.-T. Lin, Analytical approach to predict tunneling-induced subsurface settlement in sand considering soil arching effect, Comput. Geotech. 141 (2022) 104492.
[9] Cigla, M., & Ozdemir, L. (2000). *Computer modeling for improved production of mechanical excavators.* Paper presented at the SME Annual Meeting. Salt Lake City UT, USA.
[10] Engineers, Z. F. C. (2008). Final geotechnical reports of Isfahan metro line 1, Isfahan, Iran.
[11] R. Godinez, H. Yu, M. Mooney, E.A. Gharahbagh, G. Frank, Earth pressure balance machine cutterhead torque modeling: Learning from machine data. Paper Presented at the Proceedings of the Rapid Excavation and Tunneling Conference 2015, 2015.
[12] C. González, M. Arroyo, A. Gens, Thrust and torque components on mixed-face EPB drives, Tunn. Undergr. Space Technol. 57 (2016) 47–54.
[13] W. Hu, J. Rostami, Laboratory Study of Clay Clogging Issues for EPB TBM Tunneling Applications. Paper Presented at the Rapid Excavation and Tunneling Conference 2021 Proceedings, 2021.
[14] JSCE. (2016). Standard Specifications for Tunneling–2016: Shield Tunnels.
[15] Korbin, G. (1998). *Claims and tunnel boring machines: contributing factors and lessons learned.* Paper presented at the Engineering Geology: A global view from the Pacific Rim.
[16] Krause, T. (1987). Schildvortrieb mit flüssigkeits-und erdgestützter Ortsbrust. *Mitteilungen des Instituts für Grundbau und Bodenmechanik der Technischen Universität Braunschweig*(24).
[17] Y.-J. Lee, Investigation of subsurface deformations associated with model tunnels in a granular mass, Tunn. Undergr. Space Technol. 24 (6) (2009) 654–664.
[18] X. Li, L.-J. Wu, Y.-J. Wang, J.-H. Li, Rock fragmentation indexes reflecting rock mass quality based on real-time data of TBM tunnelling, Sci. Rep. 13 (1) (2023) 10420.
[19] X. Li, L.-J. Wu, Y. Wang, H. Liu, Z. Chen, L.-J. Jing, Y. Wang, A data driven real-time perception method of rock condition in TBM construction, *Can. Geotech. J.*(ja) (2023).
[20] Maidl, B., Herrenknecht, M., Maidl, U., & Wehrmeyer, G. (2012). Mechanised shield tunnelling. Berlin: Ernst W. In: & Sohn Verlag.
[21] M. Melis Maynar, Las tuneladoras de 3 carriles de la M-30. Las mayores y mas potentes jamas fabricadas, *Revista De Obras Publicas*(3.454) (2005).
[22] M. Mooney, H. Yu, S. Mokhtari, X. Zhang, X. Zhou, E. Alavi, W. Hodder, EPB TBM performance prediction on the university link U230 project. Proceedings of North American Tunneling, 2018.
[23] J. Rostami, L. Ozdemir, A new model for performance prediction of hard rock TBMs. Proceedings of the Rapid Excavation and Tunneling Conference, 1993.
[24] H. Shi, H. Yang, G. Gong, L. Wang, Determination of the cutterhead torque for EPB shield tunneling machine, Autom. Constr. 20 (8) (2011) 1087–1095.
[25] A. Toth, J. Zhao, *Evaluation of EPB TBM performance in mixed ground conditions.* Paper presented at the World Tunnel Congress (WTC)/General Assembly of the International-Tunnelling-and-Underground-Space-Association (ITA), Underground-The Way to the Future, (ITA) 2013, 2013.
[26] LinTao Wang, GuoFang Gong, H.u. Shi, HuaYong Yang, A new calculation model of cutterhead torque and investigation of its influencing factors, Sci. China Technol. Sci. 55 (6) (2012) 1581–1588.
[27] W. Wittke, C. Erichsen, J. Gattermann, Stability analysis and design for mechanized tunnelling, Geotechnical Engineering in Research and Practice 581 (2007).
[28] M. Zare Naghadehi, M. Samaei, M. Ranjbarnia, V. Nourani, State-of-the-art predictive modeling of TBM performance in changing geological conditions through gene expression programming, Measurement 126 (2018) 46–57, https://doi.org/10.1016/j.measurement.2018.05.049.
[29] N. Zhang, A. Zhou, Y. Pan, S.-L. Shen, Measurement and prediction of tunnelling-induced ground settlement in karst region by using expanding deep learning method, Measurement 183 (2021), 109700, https://doi.org/10.1016/j.measurement.2021.109700.
[30] Q. Zhang, Z. Hou, G. Huang, Z. Cai, Y. Kang, Mechanical characterization of the load distribution on the cutterhead–ground interface of shield tunneling machines, Tunn. Undergr. Space Technol. 47 (2015) 106–113.
[31] Q. Zhang, CuiXia Su, QingHua Qin, ZongXi Cai, ZhenDe Hou, YiLian Kang, Modeling and prediction for the thrust on EPB TBMs under different geological conditions by considering mechanical decoupling, Sci. China Technol. Sci. 59 (9) (2016) 1428–1434.
[32] Y.u. Zhao, Q. Gong, Z. Tian, S. Zhou, H.e. Jiang, Torque fluctuation analysis and penetration prediction of EPB TBM in rock–soil interface mixed ground, Tunn. Undergr. Space Technol. 91 (2019) 103002.
[33] X.-P. Zhou, S.-F. Zhai, Estimation of the cutterhead torque for earth pressure balance TBM under mixed-face conditions, Tunn. Undergr. Space Technol. 74 (2018) 217–229.